Received: 8 February 2023 | Revised: 12 April 2023 | Accepted: 20 April 2023

DOI: 10.1111/mec.16968

ORIGINAL ARTICLE

MOLECULAR ECOLOGY WILEY

Multisensory integration by polymodal sensory neurons dictates larval settlement in a brainless cnidarian larva

Sydney Birch[1,2] | David Plachetzki[1]

[1]Department of Molecular, Cellular, and Biomedical Sciences, University of New Hampshire, Durham, New Hampshire, USA

[2]Department of Biological Sciences, University of North Carolina at Charlotte, Charlotte, North Carolina, USA

Correspondence
Sydney Birch, Department of Molecular, Cellular, and Biomedical Sciences, University of New Hampshire, Durham, NH 03824, USA.
Email: sbirch1@uncc.edu

Funding information
National Science Foundation, Grant/Award Number: 1638296, 1755337 and Graduate Research Fellowship (GRF); U.S. Department of Agriculture, Grant/Award Number: Hatch Project 1013436

Handling Editor: John A. Benzie

Abstract

Multisensory integration (MSI) combines information from more than one sensory modality to elicit behaviours distinct from unisensory behaviours. MSI is best understood in animals with complex brains and specialized centres for parsing different modes of sensory information, but dispersive larvae of sessile marine invertebrates utilize multimodal environmental sensory stimuli to base irreversible settlement decisions on, and most lack complex brains. Here, we examined the sensory determinants of settlement in actinula larvae of the hydrozoan *Ectopleura crocea* (Cnidaria), which possess a diffuse nerve net. A factorial settlement study revealed that photo-, chemo- and mechanosensory cues each influenced the settlement response in a complex and hierarchical manner that was dependent on specific combinations of cues, an indication of MSI. Additionally, sensory gene expression over development peaked with developmental competence to settle, which in actinulae, requires cnidocyte discharge. Transcriptome analyses also highlighted several deep homological links between cnidarian and bilaterian mechano-, chemo-, and photosensory pathways. Fluorescent in situ hybridization studies of candidate transcripts suggested cellular partitioning of sensory function among the few cell types that comprise the actinula nervous system, where ubiquitous polymodal sensory neurons expressing putative chemo- and photosensitivity interface with mechanoreceptive cnidocytes. We propose a simple multisensory processing circuit, involving polymodal chemo/photosensory neurons and mechanoreceptive cnidocytes, that is sufficient to explain MSI in actinulae settlement. Our study demonstrates that MSI is not exclusive to complex brains, but likely predated and contextualized their evolution.

KEYWORDS
Cnidaria, hydrozoa, larval settlement, multisensory integration, sensory cue hierarchy

1 | INTRODUCTION

A distinguishing feature of animals is their exquisite capacity to receive sensory information from the environment and integrate it into behaviour. Animals may integrate sensory signals from individual modalities (e.g. vision or taste), or they may perform multisensory integration (MSI), which combines information from more than one modality to elicit behaviours that are distinct from those elicited by unisensory-induced behaviours (Alvarado et al., 2007; Otto et al., 2013; Stein et al., 1989, 2014; Stein & Meredith, 1993; Stevenson et al., 2014).

Multisensory integration is best understood in bilaterian animals with complex nervous systems that include specialized centers

for information processing and exchange (Currier & Nagel, 2020; Ghosh et al., 2017; Otto et al., 2013; Stein, 1998; Stein et al., 2014). Classically, MSI studies are conducted at the neuron level where neuronal signals are processed in the brain to make behavioural decisions (Meredith & Stein, 1983; Otto et al., 2013; Stein, 1998; Stein & Stanford, 2008). However, much less research has been conducted on organisms that lack complex nervous systems or brains. Moreover, zoospores of an *Allomyces* fungus utilize a multimodal system involving chemo- and phototaxis (Swafford & Oakley, 2018), suggesting the possibility that MSI may have evolved prior to the evolution of complex nervous systems.

Sensory integration is critically important for sessile marine invertebrates that utilize larvae for dispersal and to make irreversible settlement decisions. Because some sensory cues may be better indicators of site quality than others, larvae may place emphasis on select cues, leading to a hierarchy of sensory cues that determine where settlement occurs (Hodin et al., 2018; Kingsford et al., 2002; Müller & Leitz, 2002; Woodson et al., 2007). However, MSI has yet to be demonstrated in marine invertebrate larval settlement, and little is known about the potential for MSI in such organisms that lack complex nervous systems or brains.

The marine hydrozoan *Ectopleura crocea* is a benthic colonial species with a pan-global distribution in temperate coastal regions. Unlike many other cnidarian species, *E. crocea* possesses an actinula larva (Figure 1c). Actinulae are motile lecithotrophic larvae that develop in the following five stages: the star embryo, preactinula, actinula, nematocyte-printing (settling) actinula, and settled actinula. *E. crocea* actinulae begin settlement with a larval behaviour called nematocyte-printing, where they use tentacles loaded with cnidocytes to tether to the substrate, presumably in the context of suitable environmental cues (Yamashita et al., 2003). However, little is known about the sensory cues that determine this process, the cell types that receive such information, or the underlying genetic machinery of sensation that coordinates settlement decisions.

Here, we describe integrative studies on the sensory biology of settlement in actinulae of *E. crocea*. Immunohistochemical studies of larval neural network development indicate that *E. crocea* larvae first possess a defined nervous system complete with robust tentacular cnidocytes and sensory neurons by the actinula stage of development. Next, to identify the sensory cues involved in settlement, we performed a factorial larval settlement study that investigated the effects of individual and combined cues (e.g. light, chemical (biofilm), and mechanical/surface texture) corresponding to three prominent sensory modalities. We found strong evidence of MSI during larval settlement where the highest rates of settlement occurred in the presence of all three sensory cues and where the effects of cues changed in the presence or absence of other cues, resulting in a sensory cue hierarchy. Developmental transcriptome analyses revealed deep homological links with bilaterian sensory system development and a peak expression of sensory transduction components for each of the three modalities in actinula stage larvae. Lastly, RNA fluorescent in situ hybridization (FISH) studies localize several prominent sensory transcripts including opsin (photosensitivity), PKD2L1 and PKD1L3 (chemosensitivity), and ASIC, Piezo, and TRPA (mechanosensitivity) to sensory neurons and their attendant cnidocytes in settlement-competent actinulae. Our results demonstrate MSI in the brainless actinula of *E. crocea* and suggest that this capacity is facilitated by the activities of polymodal sensory neurons with distant ancestry to unimodal primary sensory neurons known from bilaterian animals.

2 | MATERIALS AND METHODS

2.1 | Field collection of *E. crocea* colonies

Larvae were obtained by collecting adult *E. crocea* colonies at the UNH Coastal Marine Lab (CML) pier in New Castle, NH in June and July 2020. Colonies were cultured and maintained in unfiltered seawater with aeration at a 12/12 L:D cycle at 18°C as per Mackie (1966). Colonies were undisturbed overnight to allow spawning and actinula release. Larvae were identified and collected the following day for settlement experiments, molecular analyses or staining.

2.2 | Immunohistochemistry and confocal microscopy

Immunohistochemistry was performed on four developmental stages: star embryos, pre-actinulae, actinula larvae and juvenile polyps. Samples were fixed overnight at 4°C in 4% paraformaldehyde (Sigma, P6148) in PBST. We followed the protocol of Plachetzki et al. (2012) with minor alterations. Samples were washed five times with 5-min incubations in PBST (3.2 mM Na2HPO4, 0.5 mM KH2PO4, 1.3 mM KCl, 135 mM NaCl, 0.1% Tween 20, pH 7.4) and blocked for 2 h in PBST +20% normal goat serum (NGS; Sigma, NS02L) at room temperature. Samples were then incubated with primary antibody, anti-acetylated α tubulin (1:500; Sigma, T6793), in blocking solution overnight at 4°C. Following the primary antibody, samples were washed five times with 5-min incubations in PBST and blocked as before. Samples were incubated with the secondary antibody, Alexa Fluor 546-conjugated anti-mouse IgG (1:1000; Life Technologies, A11030) and blocking reagent overnight at 4°C. Samples were then washed five times with 5-min incubations in PBST. Afterward, a solution containing Alexa Fluor 488-labelled phalloidin stock (1:40; Invitrogen, A12379) in PBST was added for 1 h. Samples were then washed five times with 10-min incubations and were mounted in ProLong Antifade Mountant with DAPI (ThermoFisher, P36941). Samples were imaged on a Nikon A1R HD confocal microscope.

2.3 | Experimental design of the larval settlement study and materials

The larval settlement study was designed as a 7×2×2 split-plot Randomized Complete Block Design (RCBD) with 10 blocks (Figure 2a). The blocking variable was the experimental day that

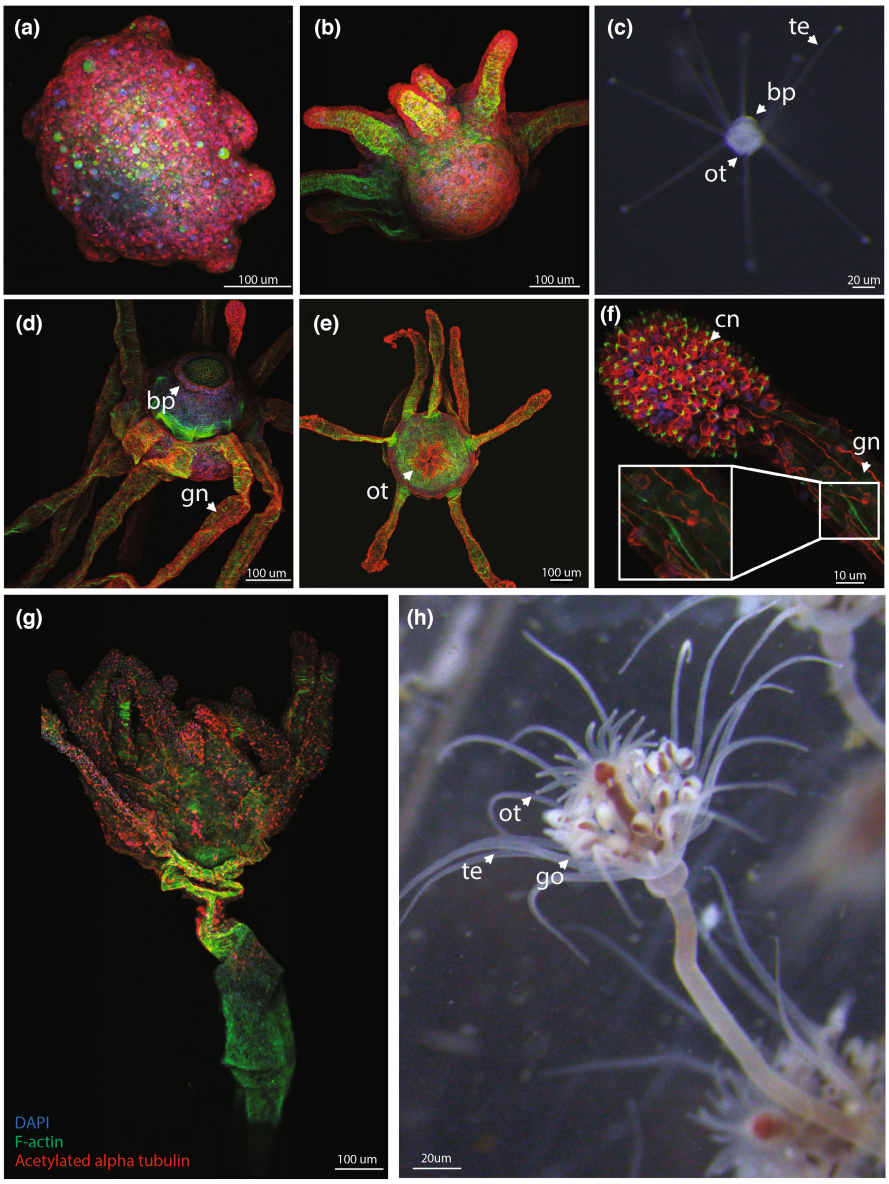

FIGURE 1 Nervous system development of *Ectopleura crocea* actinulae larvae. (a, b, d–g) Immunohistochemistry (IHC) staining of four developmental stages of *E. crocea* larvae where red staining corresponds to acetylated alpha-tubulin immunoreactivity in neural cells, green staining corresponds to contractile F-actin in muscles and stereocilia, and blue staining corresponds to DNA in nuclei. (a) Stage 1, star embryo. (b) Stage 2, preactinula. (c) Light micrograph of an actinula larva. The arrows point to the basal protrusion (bp), tentacles (te) and the developing oral tentacles (ot). (d) Aboral end of Stage 3–4 actinula larva. Arrows point to the basal protrusion (bp) and ganglion neurons (gn) in the tentacles. (e) Oral end of actinula larva at stage 3–4. The arrow is pointing to the developing oral tentacles (ot). (f) High magnification of a stage 3–4 actinula tentacle. An abundance of cnidocytes (cn) are found at the tips of the tentacles. Additionally, ganglion neurons (gn) extend down the tentacles and connect to the actinular nerve net. (g) A metamorphosed juvenile polyp. (h) A light micrograph of an adult *E. crocea* polyp. The arrows point to the oral tentacles (ot), the aboral tentacles (te) and the gonophores (go).

FIGURE 2 Settlement responses of actinula larvae to three sensory cues. (a) Cartoon depiction of the larval settlement experimental design: 7×2×2 Split-plot RCBD with 10 replicates. The block variable is an experimental day and a single replicate, depicted as a grey rectangle. All four combinations of presence/absence of biofilm and surface texture (depicted as a–d treatments) were exposed to all seven light conditions in a single block (replicate). (b) The individual effect of light cues on settlement. Larval settlement is significantly higher ($p = .0027$) in the presence of a light cue compared to the absence of a light cue (darkness). (c) The individual effect of chemical cues (biofilm) on settlement. Larval settlement is significantly higher ($p = <2e\text{-}16$) in the presence of a chemical cue compared to the absence of one. (d) The individual effect of mechanical cues (surface texture) on settlement. Larval settlement is significantly lower ($p = <2e\text{-}16$) in the presence of a mechanical cue compared to the absence of one. (e) The effect of the seven light conditions on settlement. Larval settlement was significantly lower in darkness ($p = .00272$) and in red wavelengths of light ($p = .01137$), and significantly higher in green wavelengths of light ($p = .00167$). (f) The effect of chemical cues (biofilm) across the seven light conditions. There were no significant differences in settlement in any wavelength of light (blue $p = .51$; green $p = .60$; red $p = .88$) in the presence of a chemical cue. (g) The effect of mechanical cues (surface texture) across the seven light conditions. There were no significant differences in settlement in any wavelength of light in the presence of a mechanical cue (blue $p = .99$; green $p = .79$; red $p = .79$). (h) The effect of chemical and mechanical cues combined across the seven light conditions. There was a significant increase in settlement in the presence of green wavelengths of light ($p = .02$) and significantly lower settlement in red wavelengths of light ($p = .003$). (i) The interaction of chemical cues and light cues. There was no significant interaction between these two cues ($p = .33$). (j) The interaction between mechanical cues and light cues. There was no significant interaction between these two cues ($p = .89$). (k) The interaction between chemical and mechanical cues. There was a significant interaction between these two cues ($p = <2e\text{-}16$) with an additive effect in the presence of both cues. (l) The three-way interaction of chemical, mechanical, and light cues. There is a significant three-way interaction ($p = .02$) where higher settlement rates occur in the presence of all three cues compared to other combinations.

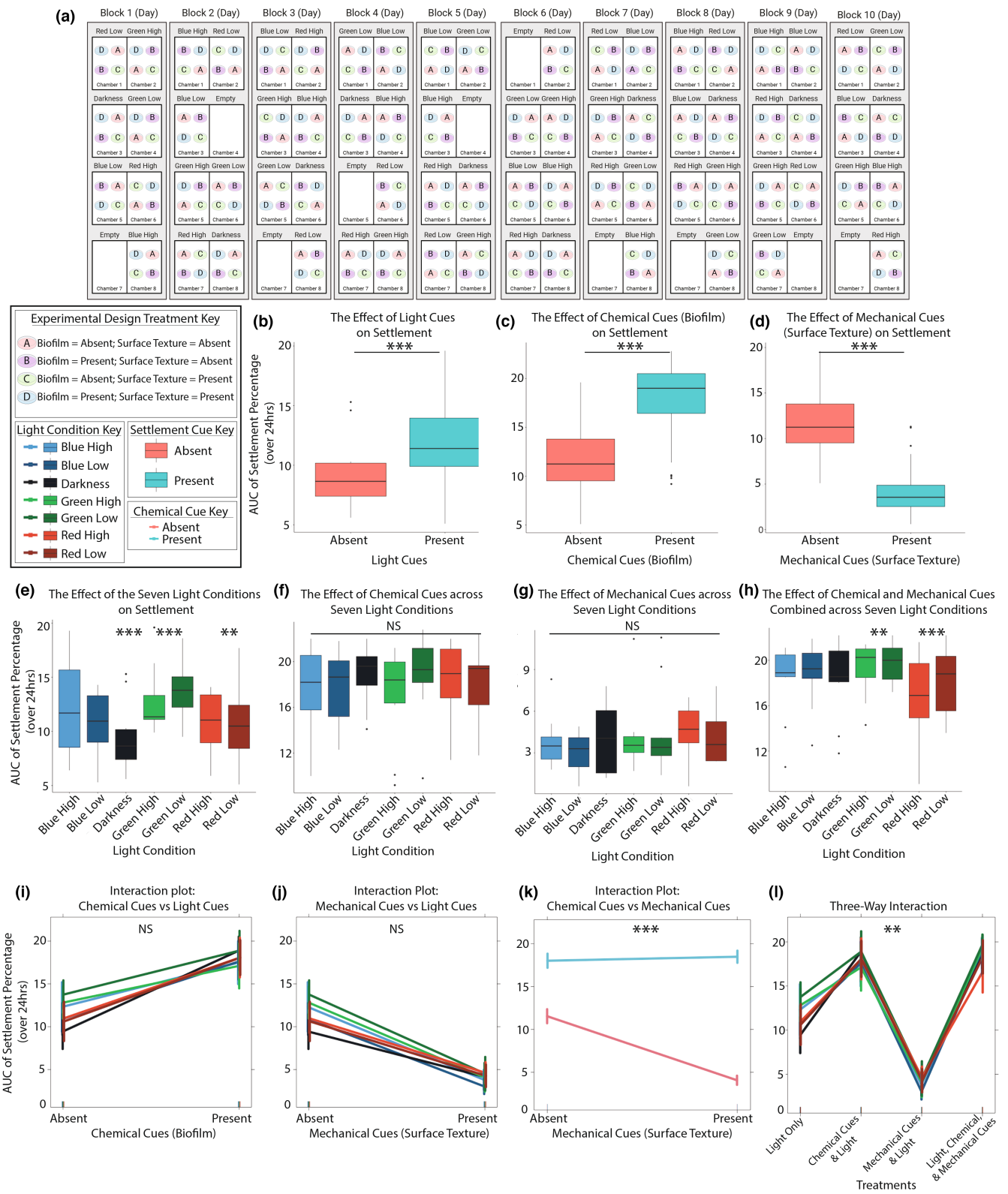

replicates were performed on, where larvae in one block were from colonies collected at the same time the day before the experiment. The blocking variable accounted for variation between colonies and days across the study, where each block contained all 28 treatments. An experimental unit was a single petri dish that contained 10 actinula larvae. We used the area under the curve (AUC) as our response variable, which was calculated with the settlement percentage. The use of AUC as our response variable allowed repeated measures to be collapsed, providing a more robust analysis while still providing information on how the settlement rate changed over

TABLE 1 The seven levels of the light condition factor with their corresponding measurements.

Light conditions in study	Wavelength (nm)	Intensity (μmol/m^2/s)
Red light, High intensity	630	10
Red light, Low intensity	630	5
Green light, High intensity	520	10
Green light, Low intensity	520	5
Blue light, High intensity	460	10
Blue light, Low intensity	460	5
Darkness	0	0

time (over seven-time points). Additionally, we considered three levels of larval metamorphosis during quantification (larval stage, settled/attached larvae, and metamorphosed juvenile polyp). The three treatment factors were the sensory cues of interest which included seven levels of light conditions including the absence of light, two levels of chemosensory treatments (presence/absence of biofilm), and two levels of mechanosensory treatments (presence/absence of surface texture). Replicates were performed in experimental chambers described below. The first randomization of the split-plot design was applied at the chamber level and entailed the assignment of the seven light conditions described in Table 1. The second randomization included the assignment of chemical and mechanical cues, which were applied at the petri-dish level in a factorial presence/absence structure (Table 2).

Experimental chambers (40.64 cm × 30.48 cm × 30.48 cm) were fabricated with black opaque acrylic (Acrylite; Extruded 9 M001; 4.49 mm thick) with two 85 mm diameter openings in the top for light fixtures (Figure S1A). An additional piece of acrylic (30.48 cm × 30.48 cm) with the same thickness was placed in the centre of the box to create two separate chambers, Figure S1B. Heatless LED lights (Super bright LEDs, part #: WRLFA-RGB6W-60) were placed in the cutouts, which allowed control of four different light intensity settings for the wavelengths red (630 nm), green (520 nm) and blue (460 nm). Light conditions were selected according to previous photosensory work on *Hydra* (Guertin & Kass-Simon, 2015; Plachetzki et al., 2012). Light intensity was measured using an LI-COR Biosciences LI-1000 DataLogger.

To obtain chemical cues, we allowed petri-dishes to generate biofilms by placing dishes in mesh bags attached to the UNH CML pier for 1 week at a depth of 1.5 m (Lee et al., 2008, 2014). The following week, Petri dishes containing natural biofilms were transported to the laboratory in seawater collected at site and were used in settlement studies immediately (Corcoll et al., 2017). To obtain mechanical stimuli, the inner surface of 100 mm × 15 mm plastic petri dishes (Thermo Scientific) were roughened prior to biofilm generation with 36-grit ceramic alumina sandpaper (Lowes; Model #: 9150–052) in a circular motion on the outer part of the dish, then with three, non-overlapping lateral motions to ensure full coverage. Dishes were rinsed in DI water and then sea water immediately prior to use.

TABLE 2 Factorial structure of chemical and mechanical cue dish treatments.

	Chemical cue absent	Chemical cue present
Mechanical cue absent	Dish Treatment A	Dish Treatment B
Mechanical cue present	Dish Treatment C	Dish Treatment D

2.4 | Larval settlement

Actinula stage larvae were collected and placed in petri dishes where each dish contained 10 larvae. Dish treatments corresponded to the predetermined randomized dish conditions for the 28 experimental treatments (Figure 2a). Larvae were identified under a microscope, following the work of Yamashita et al. (2003), where we sought out actinula with stiff tentacles, small and circular bodies and short aboral poles.

One block (replicate) of all 28 treatment conditions began once larvae were collected at the actinula stage. Metamorphic stages were recorded at 0, 2, 4, 6, 8, 12 and 24 h. Larval quantification was assessed on a presence/absence metamorphosis scale with three levels: larvae that were still in the actinula phase and had not metamorphosed or settled; larvae that had settled (attached to the substrate but had not completed metamorphosis), and larvae that had completed metamorphosis into a juvenile polyp. From this information, we then calculated the AUC using the settlement percentages at each time point, which combined the number of settled and metamorphosed larvae (# of Settled + # of Metamorphosed/total # of larvae in dish). The following equation was used to calculate the AUC (Mukherjee et al., 2010; Shaner, 1977):

$$\mathrm{AUC} = \sum_{i=1}^{n} \left[\left(y_i + y_{i+1} \right) / 2 \right] * \left[t_{i+1} - t_i \right]$$

where y_i is the proportion of settled and metamorphosed larvae at the i^{th} time point; t_i is the timepoint in hours where larvae were observed, and n is the total number of observations per petri-dish in a replicate. Normally distributed data were compared statistically by a split-plot RCBD three-way analysis of variance (ANOVA) and with orthogonal contrasts in the R environment (R Core Team, 2022).

2.5 | Library preparation, sequencing and read processing

Colonies of *E. crocea* were collected at the UNH CML pier in May and June 2019. We collected six replicates of the six developmental stages for sequencing: embryos, preactinula, actinula, settling actinula, settled actinula and metamorphosed juvenile polyps (Yamashita, 2003), where each stage had a total of 125 larvae collected. Samples were stored in RNA*later* (Thermo Fisher Scientific, AM7021) in −20°C until total RNA was extracted using the PureLink RNA Mini Kit (Thermo Fisher Scientific, Cat no. 12183018A)

according to the manufacturer's instructions and quantified using NanoDrop (Thermo Scientific). Libraries were created using 1000 ng of total RNA with the NEBNext Ultra 2 Directional RNA Library Kit following the Poly(A) mRNA Magnetic Isolation module (NEB, #E7490). Libraries were sequenced on an Illumina Hi-Seq 2000 (Novogene). Reads (Accession: PRJNA929505) were processed using custom python scripts that executed FastQC (Andrews, 2010), selected the highest quality replicate for each of the six stages, and concatenated them to generate representative R1 and R2 read files to be used in de novo reference transcriptome assembly. The Oyster River Protocol (ORP) was used for assembly, which performed read trimming, read normalization, read error correction and assembly using a multi-kmer/multi-assembler approach, merging those assemblies into one final high-quality assembly (MacManes, 2018). The ORP also produced quality metrics from TransRate and BUSCO.

2.6 | Gene expression

We used Salmon (Patro et al., 2017) to quantify transcripts and EdgeR (Chen et al., 2020) to identify differentially expressed transcripts in pairwise comparisons of the six developmental stages. Transcripts were required to have at least 10 counts-per-million to be included in our analyses (Chen et al., 2020). The calcNormFactors function was used to normalize library sizes which used a trimmed mean of *M*-values (TMM) method. A quantile-adjusted conditional maximum likelihood (qCML) method was used to estimate dispersion. Differentially expressed genes (DEGs) were identified at a *p*-value of .05 using the Benjamin-Hochberg correction.

Transcripts were translated to proteins using TransDecoder (Haas et al., 2013), and cd-hit (Li & Godzik, 2006) was used to reduce the number of duplicate protein models. The reduced actinula FASTA was then used in OrthoFinder (Emms & Kelly, 2019) analyses along with publicly available data from *Homo sapiens* (Nurk et al., 2022), *Drosophila melanogaster* (Kim et al., 2021), *Hydra magnipapillata* (https://research.nhgri.nih.gov/hydra/), *Hydractinia symbiolongicarpus* (adult and larval forms; https://research.nhgri.nih.gov/hydractinia/) and *Nematostella vectensis* (Putnam et al., 2007). Resulting orthogroups were annotated based on the human sequences present, with a specific focus on genes present in three gene sets from the Gene Set Enrichment Analysis (GSEA) (Liberzon et al., 2011, 2015; Subramanian et al., 2005): GO_Sensory_Percep_Of_Light_Stimulus, GO_Sensory_Perception_of_Chemical_Stimulus, and, GO_Sensory_Perception_of_Mechanical_Stimulus. Actinula transcripts were annotated based on shared orthogroups with human sensory genes from the above gene sets. All scripts and workflows can be found on GitHub: https://github.com/sjb1061/Actinula_Paper.

2.7 | RNA fluorescent in situ hybridization

We identified the highest expressed transcripts of selected sensory genes from the three sensory gene sets. We then designed RNA-probes for our target sequences using the Stellaris RNA FISH platform (Biosearch Technologies) with the custom probe design service following their recommendations for probe design.

Samples were stained according to the Stellaris FISH protocol (https://www.biosearchtech.com/support/resources/stellaris-protocols) with alterations to the protocol. Samples were fixed overnight at 4°C in 4% paraformaldehyde (PF; Sigma, P6148) in PBS. The following day, the samples were washed five times with 5-min incubations in PBST. Samples were then incubated in Prot K (1 μg/μL) for 10 min at room temperature. Immediately following the Prot K incubation, the solution was removed, and the samples were incubated in glycine (4 μg/μL) for 10-min at room temperature. The samples were then washed twice with 5-min incubations in PBST. The samples were fixed in 4% PF for 30-min at room temperature and washed five times with 5-min incubations in PBST. The samples were then incubated in Wash Buffer A (Biodesign, Catalog# SMF-WA1-60) for 5-min at room temperature and prehybridized using Stellaris hybridization buffer (Catalogue# SMF-HB1-10) at 37°C for 1 h. Following prehybridization, hybridization buffer containing probes (10 μL of each probe for a total of 30 μL of probe) was added and the samples were incubated at 37°C overnight in the dark. The hybridization buffer was then removed, and samples were incubated in Wash Buffer A at 37°C for 30-min in the dark. Samples were then incubated in Wash buffer B (Catalogue# SMF-WB1-20) for 5-min at room temperature in the dark. We resuspended the samples in PBST and mounted them in ProLong Antifade Mountant with DAPI (ThermoFisher). The Samples were imaged on a Nikon A1R HD confocal microscope.

3 | RESULTS

3.1 | Larval nervous systems reach full development by the actinula stage of development

The actinula stage of *E. crocea* possesses morphological and cellular features such as the basal protrusion and tentacles replete with cnidocytes, which are associated with larval settlement (Yamashita et al., 2003). However, the structure of the nervous system throughout larval development has not been described. We examined larvae at four developmental stages, including the metamorphosed juvenile polyp stage, using immunohistochemistry (IHC) and confocal microscopy (Figure 1). The state of the nervous system at the earliest stage, the star embryo (Figure 1a), appears granular and undifferentiated, which we interpret as a contiguous assemblage of neural progenitor cells (Leclère et al., 2012; Rentzsch et al., 2017). The larval nervous system becomes increasingly differentiated as development proceeds from the preactinula (Figure 1b), where we see the migration of neural progenitors from the endoderm to the ectoderm (Leclère et al., 2012), to the actinula stage (Figure 1c–f), whereupon the tentacles are loaded with neurons and cnidocytes (Figure 1f). Additionally, the basal protrusion, the structure that contacts the

substrate during settlement, contains a concentrated ring of neural cells (Figure 1d). These data are consistent with the actinula stage being the competent stage for settlement and suggest that actinulae have the capacity to integrate sensory information using the tentacles and the basal protrusion.

3.2 | Differences in the sensory environment impact larval settlement

Next, we investigated the sensory information actinula integrate during the settlement decision. We performed a factorial settlement study (Figure 2) assessing the impact of photosensory, chemosensory and mechanosensory cues on larval settlement, which we analysed using a three-way analysis of variance (ANOVA). Our experiment included 10 blocks (replicates), where each block had 28 treatments of all possible combinations of cues and examined a total of 2800 individual actinula larvae (Figure 2a). While the blocking variable, which was the experimental day, did not influence the response, larval settlement did increase as the season progressed, similar to Yamashita et al (2003; Figure S2, Table S2).

First, we examined the impacts of the three individual sensory cues on settlement. We found that each sensory cue significantly impacted settlement (Figure 2b–d; Table S1). Specifically, the rate of larval settlement increased significantly in the presence of light compared to darkness ($p = .0482$; Figure 2b), and in the presence of a chemical cue (biofilm) compared to its absence ($p = <2e\text{-}16$; Figure 2c), but decreased in the presence of a mechanical cue ($p = <2e\text{-}16$; Figure 2d) when no other cues were present.

Next, we investigated the effect of photosensory cues on settlement (light condition) in the light-only treatment (Figure 2e) using contrast analyses, since this treatment included additional dimensions compared to chemical and mechanical cues (e.g. presence/absence of light, three wavelengths and two intensities, totalling seven light conditions; Figure 2a). We found that settlement increased in the presence of light compared to darkness ($p = .0027$; Figure 2e, Table S3). Furthermore, larval settlement was significantly higher in green wavelengths of light ($p = .00167$; Figure 2e), whereas significantly lower settlement occurred in red wavelengths of light ($p = .01137$; Figure 2e). No significant interaction between light intensity and light wavelength was detected.

3.3 | Multisensory integration and a sensory cue hierarchy determine settlement in actinulae

Multisensory integration is detected by examining statistical interactions between different sensory conditions (Stein et al., 2009; Stevenson et al., 2014). Therefore, we examined the two-way and three-way interactions between sensory cues as they relate to settlement rate using a three-way ANOVA and contrasts based on our experimental approach (Figure 2a; Table S4). First, we assessed the two-way interactions beginning with the interaction between light cues and chemical cues and found no significant interaction across experiments ($p = .33$; 70 experiments total; Figure 2f,i). Similarly, no significant interaction ($p = .89$) was observed between light cues and mechanical cues (Figure 2g,j). Conversely, the combination of chemical and mechanical cues displayed a significant positive interaction ($p = <2e\text{-}16$; Figure 2k; Table S4). Alone, chemosensory cues increased larval settlement. But when combined with a mechanical cue, settlement rates were significantly enhanced revealing an additive effect when both cues are present, reversing the effect of the mechanical cue. Recall that when the chemical cue was absent, the mechanical cue had a significant negative influence on settlement rate ($p = <2e\text{-}16$; Figure 2k).

Next, we examined the three-way interaction between photo-, chemo-, and mechanosensory cues and found a significant ($p = .022$) interaction. We then assessed this interaction in the context of MSI (Stein et al., 2009) by comparing the multisensory response to the largest unisensory response. The multisensory response of settlement, which is the three-way interaction, has a significantly ($p = .024$) higher mean (mean AUC of 18.48) than the largest unisensory response (chemosensory; mean AUC of 18.01), which indicates MSI by enhancement (Figures 2h,l and 3). Among the three-way interaction, larval settlement was significantly lower in darkness when chemical and mechanical cues were present ($p = .03$; Figure 2h,l). Additionally, the rate of settlement is significantly higher in green light in the presence of chemical and mechanical cues ($p = .026$), and significantly lower in red light ($p = .003$; Figure 2h,l). This interaction can be seen in Figure 2l, which shows that green light at both intensities induces higher settlement rates under chemical, and mechanical cues, and lower settlement rates occur in red light. Together, the AUC data for the different combinations of cues depict a sensory cue hierarchy (Figure 3), where the highest rates of settlement occur in the presence of light, chemical and mechanical cues.

3.4 | Sensory gene expression peaks in competent larvae and diminishes during and after metamorphosis

To assess genetic correlates of the observed sensory response, we performed a comparative transcriptome study on six developmental stages of *E. crocea*, from star embryo to metamorphosed juvenile polyps. Illumina Hi-seq resulted in an average of 38 million reads per replicate, where we had six replicates for each of the six developmental stages. De novo transcriptome assembly resulted in an assembly with 103,929 transcripts with a TransRate score of 0.34 and a BUSCO score of 98.3%.

Gene expression for both the photo- and mechanosensory gene sets share similarities across larval development (Figure 4). First, genes involved in neurogenesis, cellular morphogenesis, and sensory cell type specification show maximum expression early in development, and peak at stage 2 of development (preactinula). Examples of these for the sensory perception of light stimulus gene set include *E. crocea* homologues of SEMA5B (axonal guidance; Gaudet

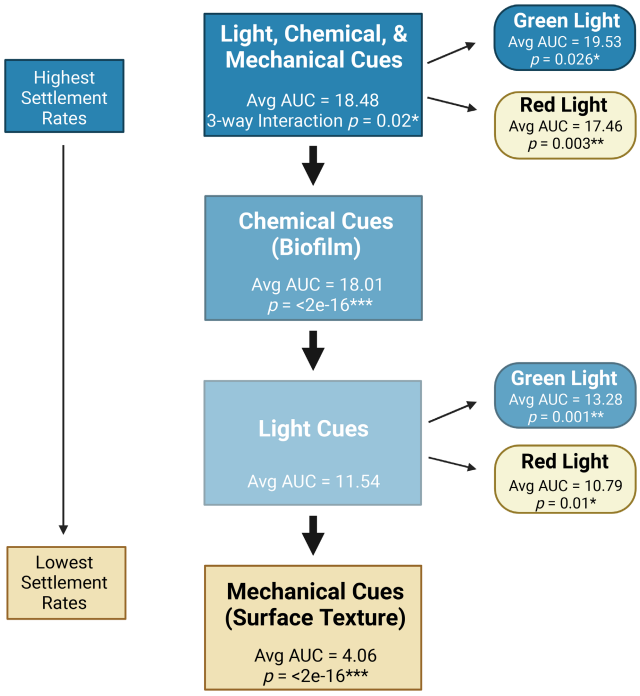

FIGURE 3 Sensory cue hierarchy of larval settlement in actinula larvae. The highest rates in settlement occur in the presence of all three cues, where significantly higher settlement rates occurred in the presence of green light, and significantly lower settlement rates occurred in the presence of red light. The second tier consists of chemical cues which significantly increases larval settlement rates, but not to the same magnitude as having all three cues present. Light did not interact with chemical cues, leading to the lack of a light hierarchy in this second tier. The third tier is the light cues only treatment, where the highest rates of settlement occur in green light and the lowest rates occur in red light. Lastly, is the Mechanical cue tier which significantly decreased settlement rates in the absence of other cues. Additionally, the scale of colour indicates the strength of a cue (darker colours indicate stronger influence).

et al., 2011; The UniProt Consortium, 2021), homologues of CRX, VSX1, VSX2 and RAX2 (transcription factors, photoreceptor specification; Mathers et al., 1997; Kimura et al., 2000), NR2E3 (transcription factor, rod specification; Peng et al., 2005), RRH (opsin, detection of light; Sun et al., 1997) and others (Figure 4a). A similar pattern is observed for the perception of mechanical stimulus gene set and includes *E.crocea* homologues of MYH14 (cell shape and cytokinesis; The UniProt Consortium, 2021), EPS8L2 (stereocilia maintenance; Offenhauser et al., 2004), DRGX (nociceptive sensory neuron development; The UniProt Consortium, 2021) and others (Figure 4c).

Next, a later pulse of gene expression associated with sensory physiology, cellular structure and morphogenesis, and another round of sensory cell type specification, characterizes both gene sets. Examples of these later expressed transcripts for the perception of light stimulus gene set include homologues of GUCY2F and RRH (phototransduction; Lowe et al., 1995; Sun et al., 1997), MYO3B (photoreceptor cell maintenance; The UniProt Consortium, 2021), ADGRV1 (development of hearing and vision; McGee et al., 2006), CNNM4 (retinal function; Parry et al., 2008), WHRN (periciliary membrane complex maintenance; Yang et al., 2010) and POU4F2 (retinal ganglion cell development; Zhang et al., 2013). Genes that peak at stages 3 and 4 (actinula) from the perception of mechanical stimulus gene set include CLIC5 (stereocilia formation; Seco et al., 2015), MYO3B (cochlear hair bundle morphogenesis), POU4F2 (terminal differentiation of hair cells), SLC25A5 (motor protein; The UniProt Consortium, 2021), ASIC2-3 (mechanoreception, potentiated by FMRFamide-related peptides; Cheng et al., 2018), TRPA1 (mechanoreceptor transduction channel; Guimaraes & Jordt, 2007) and PIEZO2 (a component of a mechanosensitive channel; Parpaite & Coste, 2017; Yan et al., 2013). Finally, transcript expression for both gene sets strongly diminish at stages 5 and 6, which corresponds to metamorphosis and the establishment of the primary polyp. This drop-off in expression is specific to the sensory gene sets used to interrogate our data and is not a general feature of the data (Figure S3, Table S5). It is noteworthy that many of the transcripts that show differential expression in development for either the photo- or mechanosensory gene sets have shared functions in both.

Similar analyses of the sensory perception of chemical stimulus gene set indicate a markedly different trend as few developmentally differentially expressed transcripts were recovered for this set (Figure 4b). However, they do indicate strong stage 4 (competent actinula) differential expression of homologues of both PKD2L1 and PKD1L3, which dimerize and facilitate sour taste perception in mammals (Fain, 2020; Ishimaru et al., 2006).

3.5 | RNA fluorescent in situ hybridization reveals evidence for polymodal sensory cells

Our studies of larval nervous system development, settlement behaviour and developmental transcriptomics portray an inflection of sensory capacity at stage 4 when actinulae are competent to settle. To elucidate the cell types associated with enhanced sensory capacity, and potential cellular partitioning among the different sensory modalities, we conducted fluorescent in situ hybridization (FISH) using RNA probes against selected, highly differentiated sensory transcripts (Figure 4) in stage 4 *E.crocea* actinulae. Our targeted transcripts include opsin (Ec_t.72976; photoreception), Piezo and TRPA1 (Ec_t.17544 and Ec_t.66269 respectively; mechanotransduction), and ASIC, PKD2L1 and PKD1L3 (Ec_t.82119, Ec_t.81080 and Ec_t.66208 respectively; chemotransduction) (Figure 4, Figure S6). We examined the cellular and spatial expression of these transcripts using the opsin probe as a reference present in all FISH experiments. Confocal optical sections (0.2 μm) indicate strong colocalization between opsin (Figure 5a–i), PKD1L3 (Figure 5a,c) PKD2L1 (Figure 5d,f,g,i), and ASIC (Figure 5a,b) in sensory neurons that are adjacent to cnidocytes in all experiments. Conversely, Piezo is strongly expressed in cnidocytes, with weaker expression of opsin also detected in cnidocytes (Figure 5g–i). Finally, opsin and PKD2L1 show some co-expression with TRPA, but most TRPA expression is observed in cnidocytes to the exclusion of PKD2L1, which is

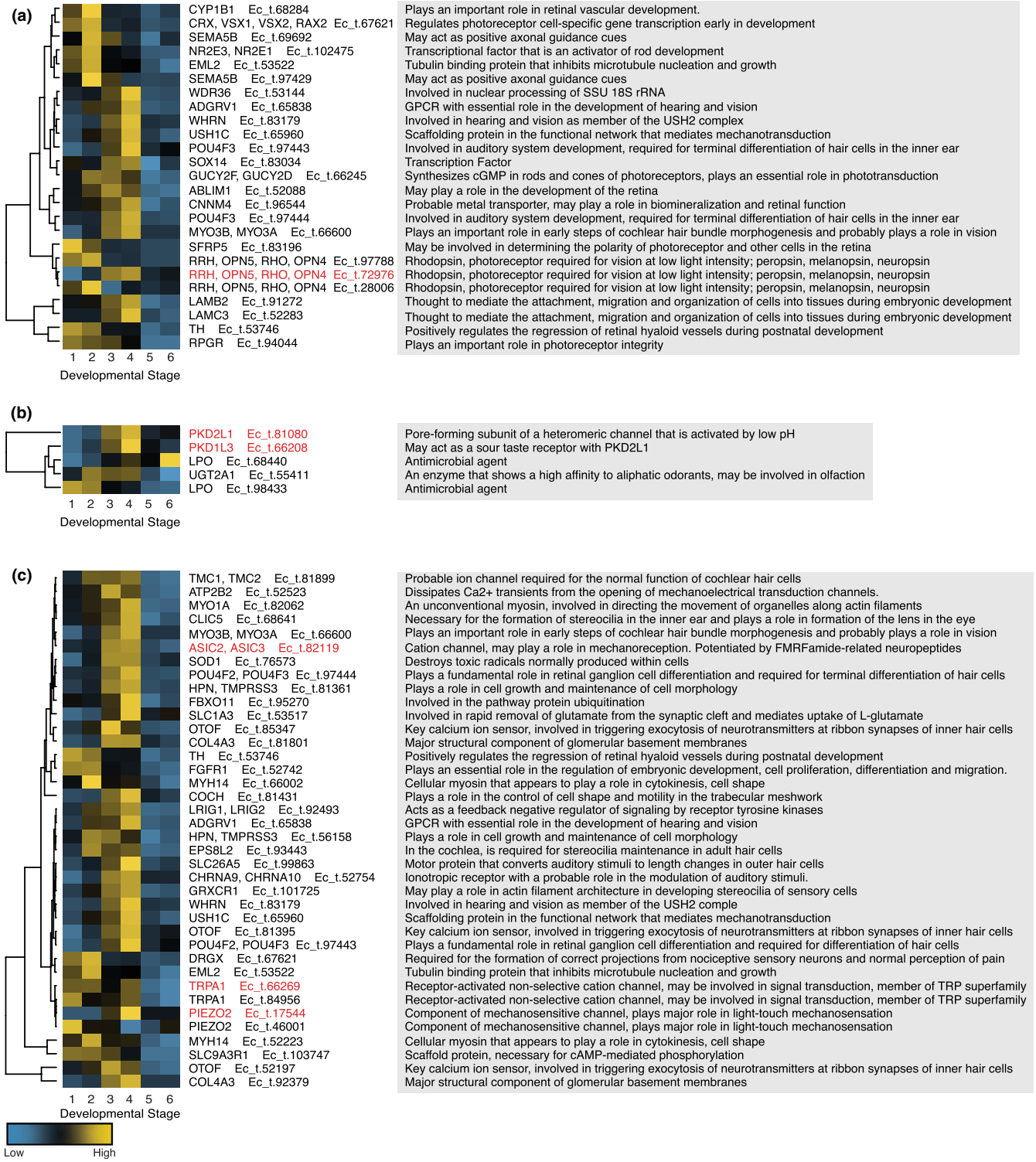

FIGURE 4 Gene expression over developmental time in actinula larvae for three sensory gene sets. Heatmaps of significantly differentially expressed genes over development for the following three gene sets: (a) sensory perception of light stimulus; (b) sensory perception of chemical stimulus; and (c) sensory perception of mechanical stimulus. High expression is signified by yellow and low expression is light blue. The grey panels to the right contain abbreviated descriptions of gene functions from The UniProt Consortium (2021). The transcripts highlighted in red are the transcripts used to make RNA Fluorescent in situ hybridization probes. Gene trees of the orthogroups of probes are given in Figure S6. Developmental stages: 1 *star embryo*, 2 *preactinula*, 3 *pre-competent actinula*, 4 *actinula in nematocyte-printing stage*, 5 *settled (attached) actinula* and 6 *metamorphosed juvenile polyp*.

expressed primarily in sensory neurons (Figure 5d–f). Our results were confirmed by quantifying colocalization using Manders' Overlap (Figure S4) and control experiments were conducted to validate expression (Figure S5). Additionally, we examined z-sections and 3D projections of confocal data to corroborate colocalization (Figures S7–S9, Video S1).

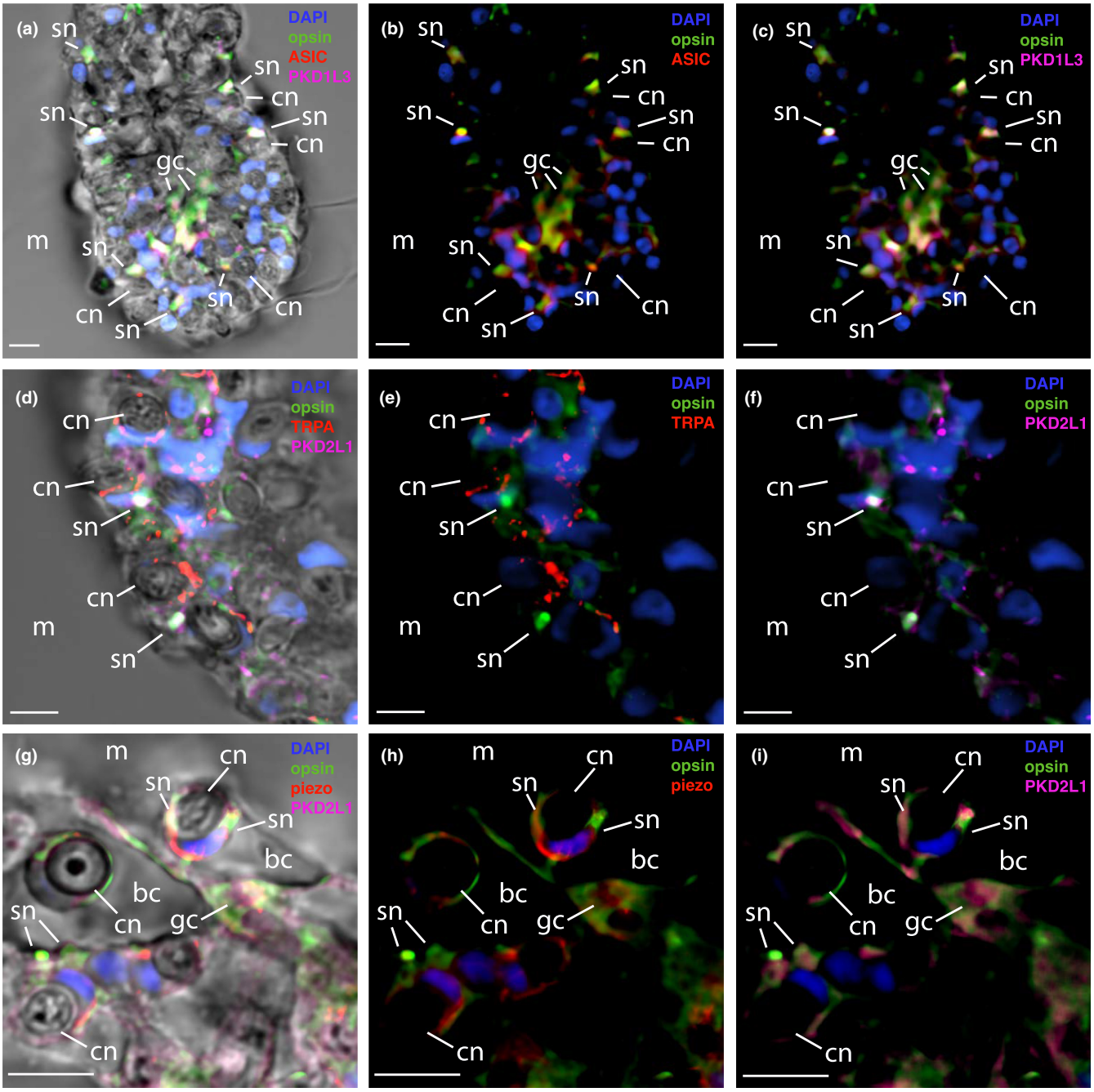

FIGURE 5 RNA fluorescent in-situ hybridizations (FISH) of sensory transcripts in actinulae tentacles. (a–c) Same tissue where green is opsin, red is ASIC, cyan is PKD1L3, and blue is DAPI. (a) Merge of all confocal channels with the transmitted light (TD) channel. (b, c) The merge of confocal channels separated from transmitted light (TD). (d–f) Same tissue where green is opsin, red is TRPA, cyan is PKD2L1, and blue is DAPI. (d) Merge of confocal channels with the transmitted light (TD) channel. (e, f) The merge of confocal channels separated from the transmitted light (TD). (g–i) Same tissue where green is opsin, red is Piezo, cyan is PKD2L1, and blue is DAPI. (g) Merge of confocal channels with the transmitted light (TD) channel. (h–i) The merge of all confocal channels separated from the transmitted light (TD). Cnidocytes (cn), sensory neurons (sn), ganglion cell (gc), battery cell (bc) and medium (sea water) (m). All scale bars are 10 μm.

4 | DISCUSSION

4.1 | Competence to settle is associated with cnidocyte and nervous system maturation

Our immunohistochemical analysis demonstrates that actinula stage larvae possess an elaborated nervous system with an abundance of cnidocytes located at the tips of the aboral tentacles. This is consistent with the findings of Yamashita et al. (2003), who described the cnidocyte complement of actinula larvae and showed that atrichous isorhizas function to temporarily attach to surfaces in a behaviour referred to as nematocyte-printing. In hydrozoans like *E. crocea*, cnidocyte discharge is modulated by adjacent sensory neurons, with which they form synapses (Anderson et al., 2004; Anderson

& Bouchard, 2009; Hobmayer et al., 1990; Plachetzki et al., 2012; Westfall, 2004; Westfall & Kinnamon, 1978). The cnidocytes that facilitate nematocyte printing are located in the tentacles, and a ring of neurons is present at the basal protrusion located on the aboral end of actinulae (Figure 1d). Studies of other cnidarian larvae (planula) have shown that the aboral region is a site for sensory integration (Matsushima et al., 2010; Schwoerer-Böhning et al., 1990; Seipp et al., 2007; Tran & Hadfield, 2013; Vandermeulen, 1974). This provides support to the hypothesis that the basal protrusion of actinulae may also be involved in sensory integration, but further research is needed. Furthermore, we propose that the sensory interplay between cnidocytes and their adjacent sensory neurons facilitate sensory integration during hydrozoan larval settlement.

4.2 | A sensory cue hierarchy and MSI during the larval settlement decision

Our larval settlement study identified a sensory cue hierarchy, where the highest rates of settlement occurred in the presence of chemical, mechanical, and light cues, with green light being the most permissive to settlement (Figure 3). This is not surprising as marine invertebrate larvae are known to integrate information from different modalities (Birch et al., 2023; Crisp, 1974; Ettinger-Epstein et al., 2008; Hadfield, 2011; Hadfield & Paul, 2001; Hodin et al., 2018; Holst & Jarms, 2007; Morello & Yund, 2016; Müller & Leitz, 2002; Pawlik, 1992; Say & Degnan, 2020; Whalan et al., 2015; Woodson et al., 2007). This type of sensory integration, and the likelihood that some cues are more important than others, was the basis for the proposal that a hierarchy of sensory cues dictates larval settlement in a species-specific manner (Ettinger-Epstein et al., 2008; Hodin et al., 2018; Kingsford et al., 2002; Woodson et al., 2007). However, the existence of such a hierarchy coupled with MSI has not been experimentally validated until now. Chemical cues produced by microbial biofilms are at the top of the hierarchy for *E. crocea* larval settlement. This is consistent with larval settlement studies in other metazoan species (e.g. annelids (Freckelton et al., 2017; Hadfield, 2011; Hadfield & Paul, 2001; Harder et al., 2002; Huang et al., 2007; Huang & Hadfield, 2003; Lau et al., 2002); cnidarians (Guo et al., 2021; Leitz & Wagner, 1993; Siboni et al., 2012, 2014; Sneed et al., 2014; Tebben et al., 2015); barnacles and bryozoans (Dobretsov & Qian, 2006; Dobretsov & Rittschof, 2020; Faimali et al., 2004; Qian et al., 2003; Zardus et al., 2008)) that identified biofilm-derived cues for larval settlement. It is likely that biofilm-derived chemical cues serve as a general indicator of habitat quality across sessile metazoan species with dispersive larval stages (Crisp, 1974; Hadfield, 2011; Lau et al., 2005; Wieczorek & Todd, 1998).

We also found a significant effect of light wavelength on larval settlement in *E. crocea*. Previous work in hydrozoan species noted similar findings where animals were more sensitive to light in the blue to blue–green spectrum compared to red light (Guertin & Kass-Simon, 2015; Plachetzki et al., 2012; Taddei-Ferretti et al., 2004). However, this differs from current evidence for anthozoan planulae where some species' planulae prefer to settle in red wavelengths of light (Foster & Gilmour, 2016; Mason et al., 2011, 2012; Mason & Cohen, 2012), while others settle across different wavelengths, suggesting species-specific preferences and a mechanism of niche differentiation (Mundy & Babcock, 1998; Strader et al., 2015). In the case of *E. crocea* larval settlement, green light, which penetrates only to shallow depths in the water column, may serve as a depth meter ensuring that colonies of *E. crocea* settle at shallow depths where prey items like plankton are abundant. We note that our finding of the preference of *E. crocea* larvae to settle in areas illuminated in green light does not in itself indicate the capacity for discrimination between wavelengths of light in *E. crocea* larvae. It is more likely that actinulae larvae are effectively "colour blind" but show a higher sensitivity to green light due to a limited photoreceptor palate with sensitivity in that range. Indeed, we uncovered only three closely related opsin transcripts from all *E. crocea* larval stages (Figure S6).

Many of the same sensory cues that we investigated here have been investigated previously in other species. However, in most cases, studies have focused on one or two cues of interest (Hodin et al., 2018; Holst & Jarms, 2007; Mason & Cohen, 2012; Nellis & Bourget, 1996; Say & Degnan, 2020; Strader et al., 2015; Svane & Dolmer, 1995; Wahab et al., 2011; Wieczorek & Todd, 1998; Zardus et al., 2008). Our factorial experimental design allowed us to identify interactions between sensory modalities and to test the possibility of MSI. Surprisingly, we found a significant interaction between mechanical (surface texture) and chemical (biofilm) cues where, in the presence of chemical cues, surface texture enhances settlement rates, but in the absence of chemical cues, surface texture is inhibitory. This significant and sign-reversing sensory interaction constitutes MSI by enhancement (Stein et al., 2009) and is likely mediated by signalling between sensory neurons and their adjacent cnidocytes. MSI by enhancement is stronger when light is present in addition to chemical and mechanical cues, suggesting that both photosensitivity and chemosensitivity have positive impacts on settlement when mechanical cues are present.

4.3 | The cellular basis for MSI in actinulae

Temporal patterns of gene expression also illuminate the sensory determinants of the settlement decision in *E. crocea*. While each of the three gene sets used for GSEA interrogation contained >200 genes, only a subset of those genes have orthologs in the *E. crocea* transcriptome and are differentially expressed between stages (Figure 4). The mechanosensory gene set includes the largest number of active genes while the chemosensory gene set contains the least number of genes. This disparity is partly due to the relative degree of conservation in gene function between cnidarian genomes and those of model organisms from which annotations are based, and partly due to genes that are differentially expressed in *E. crocea* larval development. In addition, the mechanosensory and photosensory gene sets share a number of genes in common due to pleiotropy. It is somewhat surprising that so few chemosensory genes were recovered by our screen given that chemosensitivity

is the predominant sensory cue in larval settlement. However, we did identify orthologs of both PKD1L3 and PKD2L1, which have been implicated as key components of the sour taste (pH) transduction pathway in mammals (Fain, 2020; Ishimaru et al., 2006) and have previously been implicated in cnidarian chemosensitivity (McLaughlin, 2017). Furthermore, biofilms vary in acidity (Dexter & Chandrasekaran, 2000), which could allow for the assessment of different settlement sites based on their chemosensory properties.

These analyses identify two pulses of sensory gene expression: one occurring early (stage 2, preactinula) and consisting largely of regulatory and structural factors and another occurring later (stage 4, actinula) and consisting of structural and physiological factors. These data add further support for the actinula (stage 4) as the maximally sensory-equipped larval stage and highlight candidate genes for expression analyses.

We examined the expression of several candidate genes in stage 4 actinula larvae using FISH (Figure 5). We used the same opsin transcript (Ec_t.72976) in each experiment to facilitate comparisons between genes. Our results demonstrate strong co-expression of opsin, PKD2L1, PKD1L3, and ASIC in sensory neurons. In contrast, TRPA, Piezo, and to a lesser extent, opsin transcripts localized to cnidocytes. These results demonstrate cellular partitioning between the modes of sensation, where opsin (photosensitivity) and PKD2L1, PKD1L3 and ASIC (chemosensitivity) are expressed in polymodal sensory neurons, and TRPA and Piezo (mechanosensitivity) are expressed in cnidocytes.

Together, these data suggest that MSI in *E. crocea* larval settlement is facilitated by a simple communication circuit between polymodal photo-chemosensory neurons and mechanoreceptive cnidocytes located on the tentacles. We propose that in the absence of chemical and photosensory cues, mechanosensitive cnidocytes are inhibited from discharging and little cnidocyte printing behaviour takes place. However, when light and chemical cues are present, this inhibition is relieved and mechanosensitive cnidocytes are free to fire. The combination of permissive light, chemical and mechanical cues leads to the highest rate of settlement.

MSI is best known in animals with complex brains where specialized brain centers have evolved to facilitate information processing and exchange. Here, we show that MSI is also possible in animals that lack centralized nervous systems and may be facilitated by communication between as few as two cell types: sensory neurons and cnidocytes. Moreover, given the importance of larval settlement dynamics in shaping benthic ecosystems, it is likely that MSI as observed in *E. crocea* larvae, may be an important determinant of benthic community composition and function.

5 | CONCLUSION

Understanding how cnidarians integrate sensory information from the environment is critical to understanding the ecological processes that dictate benthic community composition. At the same time, uncovering the genetic determinants of cnidarian sensory behaviour can illuminate the deep evolutionary histories of the animal senses and provide clues on their early functions. We show that brainless actinula larvae use MSI during the larval settlement decision that incorporates information processing from the light, chemical and mechanical senses. MSI is usually portrayed as a process involving information flow between higher-level brain centres (Currier & Nagel, 2020; Ghosh et al., 2017; Otto et al., 2013; Stein, 1998; Stein et al., 2014); however, our results indicate that MSI may be facilitated by interactions between cells and may have been a prominent feature of the organismal biology of metazoans prior to the evolution of complex brains.

AUTHOR CONTRIBUTIONS

Conceptualization, D.P.; methodology, D.P. and S.B.; investigation, S.B.; writing—original draft, S.B.; review & editing, D.P. and S.B.; funding acquisition, D.P.; resources, D.P.; supervision, D.P.

ACKNOWLEDGEMENTS

Partial funding was provided by the New Hampshire Agricultural Experiment Station. This work was supported by the USDA National Institute of Food and Agriculture Hatch Project 1013436 and the state of New Hampshire. In addition, SJB was supported by an NSF Graduate Research Fellowship (GRF) and DCP was supported by NSF awards 1638296 and 1755337. Research reported in this publication was also supported by the University of New Hampshire's Center for Integrated Biomedical and Bioengineering Research (CIBBR), and the School of Marine Science and Ocean Engineering's Hubbard Endowment. We are grateful to Iago Hale for the discussion and guidance on experimental design and statistics. We thank the UNH Coastal Marine Lab (CML) for the use of their research pier for animal collection.

CONFLICT OF INTEREST STATEMENT

The authors declare no conflict of interest.

DATA AVAILABILITY STATEMENT

Raw sequence reads and metadata are deposited in the SRA (BioProject PRJNA929505). All original code, bioinformatic pipelines, and outputs can be found on Github (https://github.com/sjb1061/Actinula_Paper). All behavioural analyses and metadata can be found on Github (https://github.com/sjb1061/Actinula_Paper/tree/main/Settlement_Behavior_Analysis). Raw behavioural data, RNA FISH probe sequences, and the mechanosensory pilot study can be found on Dryad (https://doi.org/10.5061/dryad.tqjq2bw3x) (Birch & Plachetzki, 2023).

ORCID

Sydney Birch https://orcid.org/0000-0003-2269-4405
David Plachetzki https://orcid.org/0000-0002-6255-7117

REFERENCES

Alvarado, J. C., Vaughan, J. W., Stanford, T. R., & Stein, B. E. (2007). Multisensory versus unisensory integration: Contrasting modes in

the superior colliculus. *Journal of Neurophysiology*, *97*, 3193–3205. https://doi.org/10.1152/jn.00018.2007

Anderson, P. A. V., & Bouchard, C. (2009). The regulation of cnidocyte discharge. *Toxicon*, *54*, 1046–1053. https://doi.org/10.1016/j.toxicon.2009.02.023

Anderson, P. A. V., Thompson, L. F., & Moneypenny, C. G. (2004). Evidence for a common pattern of peptidergic innervation of cnidocytes. *The Biological Bulletin*, *207*, 141–146.

Andrews, S. (2010). *FastQC: A quality control tool for high throughput sequence data*.

Birch and Plachetzki. (2023). *Developmental transcriptome data of Ectopleura crocea*. SRA Accession PRJNA929505 [dataset].

Birch, S., Picciani, N., Oakley, T. H., & Plachetzki, D. (2023). Cnidarians: Diversity and evolution of cnidarian visual systems. In E. Buschbeck & M. Bok (Eds.), *Distributed vision: From simple sensor to sophisticated combination eyes* (pp. 21–47). Springer.

Chen, Y., McCarthy, D., Ritchie, M., Robinson, M., & Smyth, G. (2020). edgeR: Differential analysis of sequence read count data user's guide. R Package 1–121.

Cheng, Y. R., Jiang, B. Y., & Chen, C. C. (2018). Acid-sensing ion channels: Dual function proteins for chemo-sensing and mechano-sensing. *Journal of Biomedical Science*, *25*, 1–14. https://doi.org/10.1186/s12929-018-0448-y

Corcoll, N., Österlund, T., Sinclair, L., Eiler, A., Kristiansson, E., Backhaus, T., & Eriksson, K. M. (2017). Comparison of four DNA extraction methods for comprehensive assessment of 16S rRNA bacterial diversity in marine biofilms using high-throughput sequencing. *FEMS Microbiology Letters*, *364*, 1–9. https://doi.org/10.1093/femsle/fnx139

Crisp, D. J. (1974). Factors influencing the settlement of marine invertebrate larvae. In P. Grant & A. Mackie (Eds.), *Chemoreception in marine organisms* (pp. 177–265). Academic Press.

Currier, T. A., & Nagel, K. I. (2020). Multisensory control of navigation in the fruit fly. *Current Opinion in Neurobiology*, *64*, 10–16. https://doi.org/10.1016/j.conb.2019.11.017

Dexter, S. C., & Chandrasekaran, P. (2000). Direct measurement of pH within marine biofilms on passive metals. *Biofouling*, *15*, 313–325.

Dobretsov, S., & Qian, P. Y. (2006). Facilitation and inhibition of larval attachment of the bryozoan *Bugula neritina* in association with mono-species and multi-species biofilms. *Journal of Experimental Marine Biology and Ecology*, *333*, 263–274. https://doi.org/10.1016/j.jembe.2006.01.019

Dobretsov, S., & Rittschof, D. (2020). *Love at first taste: Induction of larval settlement by marine microbes*.

Emms, D. M., & Kelly, S. (2019). OrthoFinder: Phylogenetic orthology inference for comparative genomics. *Genome Biology*, *20*, 1–14. https://doi.org/10.1186/s13059-019-1832-y

Ettinger-Epstein, P., Whalan, S., Battershill, C. N., & De Nys, R. (2008). A hierarchy of settlement cues influences larval behaviour in a coral reef sponge. *Marine Ecology Progress Series*, *365*, 103–113. https://doi.org/10.3354/meps07503

Faimali, M., Garaventa, F., Terlizzi, A., Chiantore, M., & Cattaneo-Vietti, R. (2004). The interplay of substrate nature and biofilm formation in regulating *Balanus amphitrite* Darwin, 1854 larval settlement. *Journal of Experimental Marine Biology and Ecology*, *306*, 37–50. https://doi.org/10.1016/j.jembe.2003.12.019

Fain, G. L. (2020). Taste. In *Sensory transduction* (2nd ed., pp. 159–177). Oxford University Press.

Foster, T., & Gilmour, J. P. (2016). Seeing red: Coral larvae are attracted to healthy-looking reefs. *Marine Ecology Progress Series*, *559*, 65–71. https://doi.org/10.3354/meps11902

Freckelton, M. L., Nedved, B. T., & Hadfield, M. G. (2017). Induction of invertebrate larval settlement; different bacteria, different mechanisms? *Scientific Reports*, *7*, 1–11. https://doi.org/10.1038/srep42557

Gaudet, P., Livstone, M. S., Lewis, S. E., & Thomas, P. D. (2011). Phylogenetic-based propagation of functional annotations within the gene ontology consortium. *Briefings in Bioinformatics*, *12*, 449–462. https://doi.org/10.1093/bib/bbr042

Ghosh, D. D., Nitabach, M. N., Zhang, Y., & Harris, G. (2017). Multisensory integration in *C. elegans*. *Current Opinion in Neurobiology*, *43*, 110–118. https://doi.org/10.1016/j.conb.2017.01.005

Guertin, S., & Kass-Simon, G. (2015). Extraocular spectral photosensitivity in the tentacles of *Hydra vulgaris*. *Comparative Biochemistry and Physiology. Part A, Molecular & Integrative Physiology*, *184*, 163–170. https://doi.org/10.1016/j.cbpa.2015.02.016

Guimaraes, M. Z. P., & Jordt, S. E. (2007). TRPA1: A sensory channel of many talents. In W. B. Liedtke & S. Heller (Eds.), *TRP ion channel function in sensory transduction and cellular signaling cascades*. Taylor & Francis.

Guo, H., Rischer, M., Westermann, M., & Beemelmanns, C. (2021). Two distinct bacterial biofilm components trigger metamorphosis in the colonial hydrozoan *Hydractinia echinata*. *mBio*, *12*, e0040121. https://doi.org/10.1128/mBio.00401-21

Haas, B. J., Papanicolaou, A., Yassour, M., Grabherr, M., Blood, P. D., Bowden, J., Couger, M. B., Eccles, D., Li, B., Macmanes, M. D., Ott, M., Orvis, J., Pochet, N., Strozzi, F., Weeks, N., Westerman, R., William, T., Dewey, C. N., Henschel, R., … Regev, A. (2013). De novo transcript sequence reconstruction from RNA-Seq: reference generation and analysis with trinity.

Hadfield, M., & Paul, V. (2001). Natural chemical cues for settlement and metamorphosis of marine-invertebrate larvae.

Hadfield, M. G. (2011). Biofilms and marine invertebrate larvae: What bacteria produce that larvae use to choose settlement sites. *Annual Review of Marine Science*, *3*, 453–470. https://doi.org/10.1146/annurev-marine-120709-142753

Harder, T., Lau, S. C. K., Dahms, H. U., & Qian, P. Y. (2002). Isolation of bacterial metabolites as natural inducers for larval settlement in the marine polychaete *Hydroides elegans* (HASWELL). *Journal of Chemical Ecology*, *28*, 2029–2043. https://doi.org/10.1023/A:1020702028715

Hobmayer, E., Holstein, T. W., & David, C. N. (1990). Tentacle morphogenesis in hydra. II. Formation of a complex between a sensory nerve cell and a battery cell. *Development*, *109*, 897–904. https://doi.org/10.1242/dev.109.4.897

Hodin, J., Ferner, M., Heyland, A., & Gaylord, B. (2018). I feel that! Fluid dynamics and sensory aspects of larval settlement across scales. In T. J. Carrier, A. M. Reitzel, & A. Heyland (Eds.), *Evolutionary ecology of marine invertebrate larvae* (pp. 190–207). Oxford University Press.

Holst, S., & Jarms, G. (2007). Substrate choice and settlement preferences of planula larvae of five Scyphozoa (Cnidaria) from German Bight, North Sea. *Marine Biology*, *151*, 863–871. https://doi.org/10.1007/s00227-006-0530-y

Huang, S., & Hadfield, M. G. (2003). Composition and density of bacterial biofilms determine larval settlement of the polychaete *Hydroides elegans*. *Marine Ecology Progress Series*, *260*, 161–172. https://doi.org/10.3354/meps260161

Huang, Y. L., Dobretsov, S., Xiong, H., & Qian, P. Y. (2007). Effect of biofilm formation by *Pseudoalteromonas spongiae* on induction of larval settlement of the polychaete *Hydroides elegans*. *Applied and Environmental Microbiology*, *73*, 6284–6288. https://doi.org/10.1128/AEM.00578-07

Ishimaru, Y., Inada, H., Kubota, M., Zhuang, H., Tominaga, M., & Matsunami, H. (2006). Transient receptor potential family members PKD1L3 and PKD2L1 form a candidate sour taste receptor. *Proceedings of the National Academy of Sciences of the United States of America*, *103*, 12569–12574. https://doi.org/10.1073/pnas.0602702103

Kim, B. Y., Wang, J. R., Miller, D. E., Barmina, O., Delaney, E., Thompson, A., Comeault, A. A., Peede, D., D'Agostino, E. R. R., Pelaez, J., Aguilar, J. M., Haji, D., Matsunaga, T., Armstrong, E. E., Zych, M., Ogawa, Y., Stamenković-Radak, M., Jelić, M., Veselinović, M. S., …

Petrov, D. A. (2021). Highly contiguous assemblies of 101 drosophilid genomes. *eLife*, *10*, 1–33. https://doi.org/10.7554/eLife.66405

Kimura, A., Singh, D., Wawrousek, E. F., Kikuchi, M., Nakamura, M., & Shinohara, T. (2000). Both PCE-1/RX and OTX/CRX interactions are necessary for photoreceptor- specific gene expression. *The Journal of Biological Chemistry*, *275*, 1152–1160. https://doi.org/10.1074/jbc.275.2.1152

Kingsford, M. J., Leis, J. M., Shanks, A., Lindeman, K. C., Morgan, S. G., & Pineda, J. (2002). Sensory environments, larval abilities and local self-recruitment. *Bulletin of Marine Science*, *70*, 309–340.

Lau, S. C. K., Mak, K. K. W., Chen, F., & Qian, P. Y. (2002). Bioactivity of bacterial strains isolated from marine biofilms in Hong Kong waters for the induction of larval settlement in the marine polychaete *Hydroides elegans*. *Marine Ecology Progress Series*, *226*, 301–310. https://doi.org/10.3354/meps226301

Lau, S. C. K., Thiyagarajan, V., Cheung, S. C. K., & Qian, P. Y. (2005). Roles of bacterial community composition in biofilms as a mediator for larval settlement of three marine invertebrates. *Aquatic Microbial Ecology*, *38*, 41–51. https://doi.org/10.3354/ame038041

Leclère, L., Jager, M., Barreau, C., Chang, P., le Guyader, H., Manuel, M., & Houliston, E. (2012). Maternally localized germ plasm mRNAs and germ cell/stem cell formation in the cnidarian Clytia. *Developmental Biology*, *364*, 236–248. https://doi.org/10.1016/j.ydbio.2012.01.018

Lee, J. W., Nam, J. H., Kim, Y. H., Lee, K. H., & Lee, D. H. (2008). Bacterial communities in the initial stage of marine biofilm formation on artificial surfaces. *Journal of Microbiology*, *46*, 174–182. https://doi.org/10.1007/s12275-008-0032-3

Lee, O. O., Chung, H. C., Yang, J., Wang, Y., Dash, S., Wang, H., & Qian, P. Y. (2014). Molecular techniques revealed highly diverse microbial communities in natural marine biofilms on polystyrene dishes for invertebrate larval settlement. *Microbial Ecology*, *68*, 81–93. https://doi.org/10.1007/s00248-013-0348-3

Leitz, T., & Wagner, T. (1993). The marine bacterium *Alteromonas espejiana* induces metamorphosis of the hydroid *Hydractinia echinata*. *Marine Biology*, *115*, 173–178. https://doi.org/10.1007/BF00346332

Li, W., & Godzik, A. (2006). Cd-hit: A fast program for clustering and comparing large sets of protein or nucleotide sequences. *Bioinformatics*, *22*, 1658–1659. https://doi.org/10.1093/bioinformatics/btl158

Liberzon, A., Birger, C., Thorvaldsdóttir, H., Ghandi, M., Mesirov, J. P., & Tamayo, P. (2015). The molecular signatures database Hallmark gene set collection. *Cell Systems*, *1*, 417–425. https://doi.org/10.1016/j.cels.2015.12.004

Liberzon, A., Subramanian, A., Pinchback, R., Thorvaldsdóttir, H., Tamayo, P., & Mesirov, J. P. (2011). Molecular signatures database (MSigDB) 3.0. *Bioinformatics*, *27*, 1739–1740. https://doi.org/10.1093/bioinformatics/btr260

Lowe, D. G., Dizhoor, A. M., Liu, K., Gu, Q., Spencer, M., Laura, R., Lu, L., & Hurley, J. B. (1995). Cloning and expression of a second photoreceptor-specific membrane retina guanylyl cyclase (RetGC), RetGC-2. *Proceedings of the National Academy of Sciences of the United States of America*, *92*, 5535–5539. https://doi.org/10.1073/pnas.92.12.5535

Mackie, G. O. (1966). Growth of the hydroid Tubularia in culture. In W. J. Rees (Ed.), *The Cnidaria and their evolution* (pp. 397–412). Academic Press.

MacManes, M. D. (2018). The Oyster River Protocol: A multi-assembler and kmer approach for de novo transcriptome assembly. *PeerJ*, *6*, e5428. https://doi.org/10.7717/peerj.5428

Mason, B., Beard, M., & Miller, M. W. (2011). Coral larvae settle at a higher frequency on red surfaces. *Coral Reefs*, *30*, 667–676. https://doi.org/10.1007/s00338-011-0739-1

Mason, B., Schmale, M., Gibbs, P., Miller, M. W., Wang, Q., Levay, K., Shestopalov, V., & Slepak, V. Z. (2012). Evidence for multiple phototransduction pathways in a reef-building coral. *PLoS One*, *7*, 1–9. https://doi.org/10.1371/journal.pone.0050371

Mason, B. M., & Cohen, J. H. (2012). Long-wavelength photosensitivity in coral planula larvae. *The Biological Bulletin*, *222*, 88–92. https://doi.org/10.1086/BBLv222n2p88

Mathers, P. H., Grinberg, A., Mahon, K. A., & Jamrich, M. (1997). The Rx homeobox gene is essential for vertebrate eye development. *Nature*, *387*, 603–607. https://doi.org/10.1038/42475

Matsushima, K., Kiyomoto, M., & Hatta, M. (2010). Aboral localization of responsiveness to a metamorphic neuropeptide in the planula larva of *Acropora tenuis*. *Galaxea Journal of Coral Reef Studies*, *12*, 77–81. https://doi.org/10.3755/galaxea.12.77

McGee, J. A., Goodyear, R. J., McMillan, D. R., Stauffer, E. A., Holt, J. R., Locke, K. G., Birch, D. G., Legan, P. K., White, P. C., Walsh, E. J., & Richardson, G. P. (2006). The very large G-protein-coupled receptor VLGR1: A component of the ankle link complex required for the normal development of auditory hair bundles. *The Journal of Neuroscience*, *26*, 6543–6553. https://doi.org/10.1523/JNEUROSCI.0693-06.2006

McLaughlin, S. (2017). Evidence that polycystins are involved in hydra cnidocyte discharge. *Invertebrate Neuroscience*, *17*, 1–14. https://doi.org/10.1007/s10158-016-0194-3

Meredith, M. A., & Stein, B. E. (1983). Interactions among converging sensory inputs in the superior colliculus. *Science*, *221*, 389–391.

Morello, S. L., & Yund, P. O. (2016). Response of competent blue mussel (*Mytilus edulis*) larvae to positive and negative settlement cues. *Journal of Experimental Marine Biology and Ecology*, *480*, 8–16. https://doi.org/10.1016/j.jembe.2016.03.019

Mukherjee, A. K., Mohapatra, N. K., & Nayak, P. (2010). Estimation of area under the disease progress curves in a rice-blast pathosystem from two data points. *European Journal of Plant Pathology*, *127*, 33–39. https://doi.org/10.1007/s10658-009-9568-2

Müller, W. A., & Leitz, T. (2002). Metamorphosis in the Cnidaria. *Canadian Journal of Zoology*, *80*, 1755–1771. https://doi.org/10.1139/z02-130

Mundy, C. N., & Babcock, R. C. (1998). Role of light intensity and spectral quality in coral settlement: Implications for depth-dependent settlement? *Journal of Experimental Marine Biology and Ecology*, *223*, 235–255. https://doi.org/10.1016/S0022-0981(97)00167-6

Nellis, P., & Bourget, E. (1996). Influence of physical and chemical factors on settlement and recruitment of the hydroid *Tubularia larynx*. *Marine Ecology Progress Series*, *140*, 123–139. https://doi.org/10.3354/meps140123

Nurk, S., Koren, S., Rhie, A., Rautiainen, M., Bzikadze, A. V., Mikheenko, A., Vollger, M. R., Altemose, N., Uralsky, L., Gershman, A., Aganezov, S., Hoyt, S. J., Diekhans, M., Logsdon, G. A., Alonge, M., Antonarakis, S. E., Borchers, M., Bouffard, G. G., Brooks, S. Y., … Phillippy, A. M. (2022). The complete sequence of a human genome. *Science*, *376*(6588), 44–53. https://doi.org/10.1126/science.abj6987

Offenhauser, N., Borgonovo, A., Disanza, A., Romano, P., Ponzanelli, I., Iannolo, G., Di Fiore, P. P., & Scita, G. (2004). The eps8 family of proteins links growth factor stimulation to Actin reorganization generating functional. *Molecular Biology of the Cell*, *15*, 91–98. https://doi.org/10.1091/mbc.E03

Otto, T. U., Dassy, B., & Mamassian, P. (2013). Principles of multisensory behavior. *The Journal of Neuroscience*, *33*, 7463–7474. https://doi.org/10.1523/JNEUROSCI.4678-12.2013

Parpaite, T., & Coste, B. (2017). Piezo channels. *Current Biology*, *27*, R250–R252. https://doi.org/10.1016/j.cub.2017.01.048

Parry, D. A., Mighell, A. J., El-Sayed, W., Shore, R. C., Jalili, I. K., Dollfus, H., Bloch-Zupan, A., Carlos, R., Carr, I. M., Downey, L. M., Blain, K. M., Mansfield, D. C., Shahrabi, M., Heidari, M., Aref, P., Abbasi, M., Michaelides, M., Moore, A. T., Kirkham, J., & Kirkham, C. F. (2008). Mutations in CNNM4 cause Jalili syndrome, consisting of autosomal-recessive cone-rod dystrophy and amelogenesis imperfecta. *American Journal of Human Genetics*, *84*, 266–273. https://doi.org/10.1016/j.ajhg.2009.01.009

Patro, R., Duggal, G., Love, M. I., Irizarry, R. A., & Kingsford, C. (2017). Salmon: Fast and bias-aware quantification of transcript expression using dual-phase inference. *Nature Methods*, *14*, 417–419. https://doi.org/10.1038/nmeth.4197.Salmon

Pawlik, J. R. (1992). Chemical ecology of the settlement of benthic marine-invertebrates. *Oceanography and Marine Biology*, *30*, 273–335.

Peng, G. H., Ahmad, O., Ahmad, F., Liu, J., & Chen, S. (2005). The photoreceptor-specific nuclear receptor Nr2e3 interacts with Crx and exerts opposing effects on the transcription of rod versus cone genes. *Human Molecular Genetics*, *14*, 747–764. https://doi.org/10.1093/hmg/ddi070

Plachetzki, D. C., Fong, C. R., & Oakley, T. H. (2012). Cnidocyte discharge is regulated by light and opsin-mediated phototransduction. *BMC Biology*, *10*, 1–10. https://doi.org/10.1186/1741-7007-10-17

Putnam, N. H., Srivastava, M., Hellsten, U., Dirks, B., Chapman, J., Salamov, A., Terry, A., Shapiro, H., Lindquist, E., Kapitonov, V. V., Jurka, J., Genikhovich, G., Grigoriev, I. V., Lucas, S. M., Steele, R. E., Finnerty, J. R., Technau, U., Martindale, M. Q., & Rokhsar, D. S. (2007). Sea anemone genome reveals ancestral eumetazoan gene repertoire and genomic organization. *Science*, *317*, 86–94.

Qian, P. Y., Thiyagarajan, V., Lau, S. C. K., & Cheung, S. C. K. (2003). Relationship between bacterial community profile in biofilm and attachment of the acorn barnacle *Balanus amphitrite*. *Aquatic Microbial Ecology*, *33*, 225–237. https://doi.org/10.3354/ame033225

R Core Team. (2022). *R: A language and environment for statistical computing*. R Foundation for Statistical Computing. https://www.R-project.org/

Rentzsch, F., Layden, M., & Manuel, M. (2017). The cellular and molecular basis of cnidarian neurogenesis. *Wiley Interdisciplinary Reviews: Developmental Biology*, *6*, 1–19. https://doi.org/10.1002/wdev.257

Say, T. E., & Degnan, S. M. (2020). Molecular and behavioural evidence that interdependent photo- and chemosensory systems regulate larval settlement in a marine sponge. *Molecular Ecology*, *29*, 247–261. https://doi.org/10.1111/mec.15318

Schwoerer-Böhning, B., Kroiher, M., & Müller, W. A. (1990). Signal transmission and covert prepattern in the metamorphosis of *Hydractinia echinata* (hydrozoa). *Roux's Archives of Developmental Biology*, *198*, 245–251. https://doi.org/10.1007/BF00377390

Seco, C. Z., Oonk, A. M. M., Domínguez-Ruiz, M., Draaisma, J. M. T., Gandía, M., Oostrik, J., Neveling, K., Kunst, H. P. M., Hoefsloot, L. H., del Castillo, I., Pennings, R. J. E., Kremer, H., Admiraal, R. J. C., & Schraders, M. (2015). Progressive hearing loss and vestibular dysfunction caused by a homozygous nonsense mutation in CLIC5. *European Journal of Human Genetics*, *23*, 189–194. https://doi.org/10.1038/ejhg.2014.83

Seipp, S., Schmich, J., Kehrwald, T., & Leitz, T. (2007). Metamorphosis of *Hydractinia echinata* – Natural versus artificial induction and developmental plasticity. *Development Genes and Evolution*, *217*, 385–394. https://doi.org/10.1007/s00427-007-0151-6

Shaner, G. (1977). The effect of nitrogen fertilization on the expression of slow-mildewing resistance in Knox wheat. *Phytopathology*, *77*, 1051. https://doi.org/10.1094/phyto-67-1051

Siboni, N., Abrego, D., Motti, C. A., Tebben, J., & Harder, T. (2014). Gene expression patterns during the early stages of chemically induced larval metamorphosis and settlement of the coral *Acropora millepora*. *PLoS One*, *9*, e91082. https://doi.org/10.1371/journal.pone.0091082

Siboni, N., Abrego, D., Seneca, F., Motti, C. A., Andreakis, N., Tebben, J., Blackall, L. L., & Harder, T. (2012). Using bacterial extract along with differential gene expression in *Acropora millepora* larvae to decouple the processes of attachment and metamorphosis. *PLoS One*, *7*, e37774. https://doi.org/10.1371/journal.pone.0037774

Sneed, J. M., Sharp, K. H., Ritchie, K. B., & Paul, V. J. (2014). The chemical cue tetrabromopyrrole from a biofilm bacterium induces settlement of multiple Caribbean corals. *Proceedings of the Royal Society B: Biological Sciences*, *281*, 1–9. https://doi.org/10.1098/rspb.2013.3086

Stein, B. E. (1998). Neural mechanisms for synthesizing sensory information and producing adaptive behaviors. *Experimental Brain Research*, *123*, 124–135. https://doi.org/10.1007/s002210050553

Stein, B. E., & Meredith, M. A. (1993). *The merging of the senses*. The MIT Press.

Stein, B. E., Meredith, M. A., Huneycutt, W. S., & McDade, L. (1989). Behavioral indices of multisensory integration: Orientation to visual cues is affected by auditory stimuli. *Journal of Cognitive Neuroscience*, *1*, 12–24. https://doi.org/10.1162/jocn.1989.1.1.12

Stein, B. E., & Stanford, T. R. (2008). Multisensory integration: Current issues from the perspective of the single neuron. *Nature Reviews. Neuroscience*, *9*, 406. https://doi.org/10.1038/nrn2377

Stein, B. E., Stanford, T. R., Ramachandran, R., Perrault, T. J., Jr., & Rowland, B. A. (2009). Challenges in quantifying multisensory integration: Alternative criteria, models, and inverse effectiveness. *Experimental Brain Research*, *198*, 113–126. https://doi.org/10.1007/s00221-009-1880-8

Stein, B. E., Stanford, T. R., & Rowland, B. A. (2014). Development of multisensory integration from the perspective of the individual neuron. *Nature Reviews. Neuroscience*, *15*, 520–535. https://doi.org/10.1038/nrn3742

Stevenson, R. A., Ghose, D., Fister, J. K., Sarko, D. K., Altieri, N. A., Nidiffer, A. R., Kurela, L. A. R., Siemann, J. K., James, T. W., & Wallace, M. T. (2014). Identifying and quantifying multisensory integration: A tutorial review. *Brain Topography*, *27*, 707–730. https://doi.org/10.1007/s10548-014-0365-7

Strader, M. E., Davies, S. W., & Matz, M. V. (2015). Differential responses of coral larvae to the colour of ambient light guide them to suitable settlement microhabitat. *Royal Society Open Science*, *2*, 150358. https://doi.org/10.1098/rsos.150358

Subramanian, A., Tamayo, P., Mootha, V. K., Mukherjee, S., Ebert, B. L., Gillette, M. A., Paulovich, A., Pomeroy, S. L., Golub, T. R., Lander, E. S., & Mesirov, J. P. (2005). Gene set enrichment analysis: A knowledge-based approach for interpreting genome-wide expression profiles. *Proceedings of the National Academy of Sciences of the United States of America*, *102*, 15545–15550. https://doi.org/10.1073/pnas.0506580102

Sun, H., Gilbert, D. J., Copeland, N. G., Jenkins, N. A., & Nathans, J. (1997). Peropsin, a novel visual pigment-like protein located in the apical microvilli of the retinal pigment epithelium. *Proceedings of the National Academy of Sciences of the United States of America*, *94*, 9893–9898. https://doi.org/10.1073/pnas.94.18.9893

Svane, I., & Dolmer, P. (1995). Perception of light at settlement: A comparative study of two invertebrate larvae, a scyphozoan planula and a simple ascidian tadpole. *Journal of Experimental Marine Biology and Ecology*, *187*, 51–61. https://doi.org/10.1016/0022-0981(94)00171-9

Swafford, A. J. M., & Oakley, T. H. (2018). Multimodal sensorimotor system in unicellular zoospores of a fungus. *J Exp Biol*, *221*(2), jeb163196. https://doi.org/10.1242/jeb.163196

Taddei-Ferretti, C., Musio, C., Santillo, S., & Cotugno, A. (2004). The photobiology of Hydra's periodic activity. *Hydrobiologia*, *530–531*, 129–134. https://doi.org/10.1007/s10750-004-2680-6

Tebben, J., Motti, C. A., Siboni, N., Tapiolas, D. M., Negri, A. P., Schupp, P. J., Kitamura, M., Hatta, M., Steinberg, P. D., & Harder, T. (2015). Chemical mediation of coral larval settlement by crustose coralline algae. *Scientific Reports*, *5*, 1–11. https://doi.org/10.1038/srep10803

The UniProt Consortium. (2021). UniProt: The universal protein knowledgebase in 2021. *Nucleic Acids Research*, *49*, D480–D489.

Tran, C., & Hadfield, M. G. (2013). Localization of sensory mechanisms utilized by coral planulae to detect settlement cues. *Invertebrate Biology*, *132*, 195–206. https://doi.org/10.1111/ivb.12025

Vandermeulen, J. H. (1974). Studies on reef corals. II. Fine structure of planktonic planula larva of *Pocillopora damicornis*, with emphasis on the aboral epidermis. *Marine Biology*, *27*, 239–249. https://doi.org/10.1007/BF00391949

Wahab, M. A. A., de Nys, R., & Whalan, S. (2011). Larval behaviour and settlement cues of a brooding coral reef sponge. *Coral Reefs*, *30*, 451–460. https://doi.org/10.1007/s00338-011-0727-5

Westfall, J. A. (2004). Neural pathways and innervation of cnidocytes in tentacles of sea anemones. *Hydrobiologia*, *530–531*, 117–121. https://doi.org/10.1007/s10750-004-2678-0

Westfall, J. A., & Kinnamon, J. C. (1978). A second sensory-motor-interneuron with neurosecretory granules in hydra. *Journal of Neurocytology*, *7*, 365–379. https://doi.org/10.1007/BF01176999

Whalan, S. A., Wahab, M. A., Sprungala, S., Poole, A. J., & De Nys, R. (2015). Larval settlement: The role of surface topography for sessile coral reef invertebrates. *PLoS One*, *10*, 1–17. https://doi.org/10.1371/journal.pone.0117675

Wieczorek, S. K., & Todd, C. D. (1998). Inhibition and facilitation of settlement of epifaunal marine invertebrate larvae by microbial biofilm cues. *Biofouling*, *12*, 81–118. https://doi.org/10.1080/08927019809378348

Woodson, C. B., Webster, D. R., Weissburg, M. J., & Yen, J. (2007). Cue hierarchy and foraging in calanoid copepods: Ecological implications of oceanographic structure. *Marine Ecology Progress Series*, *330*, 163–177. https://doi.org/10.3354/meps330163

Yamashita, K. (2003). Larval behavioral, morphological changes, and nematocyte dynamics during settlement of actinulae of *Tubularia mesembryanthemum*, Allman 1871 (Hydrozoa: Tubulariidae). *The Biological Bulletin*, *204*, 256–269.

Yan, Z., Zhang, W., He, Y., Gorczyca, D., Xiang, Y., Cheng, L. E., Meltzer, S., Jan, L. Y., & Jan, Y. N. (2013). Drosophila NOMPC is a mechanotransduction channel subunit for gentle-touch sensation. *Nature*, *493*, 221–225. https://doi.org/10.1038/nature11685

Yang, J., Liu, X., Zhao, Y., Adamian, M., Pawlyk, B., Sun, X., McMillan, D., Liberman, M. C., & Li, T. (2010). Ablation of whirlin long isoform disrupts the USH2 protein complex and causes vision and hearing loss. *PLoS Genetics*, *6*, 9. https://doi.org/10.1371/journal.pgen.1000955

Zardus, J. D., Nedved, B. T., Huang, Y., Tran, C., & Hadfield, M. G. (2008). Microbial biofilms facilitate adhesion in biofouling invertebrates. *The Biological Bulletin*, *214*, 91–98. https://doi.org/10.2307/25066663

Zhang, L., Wahlin, K., Li, Y., Masuda, T., Yang, Z., Zack, D. J., & Esumi, N. (2013). RIT2, a neuron-specific small guanosine triphosphatase, is expressed in retinal neuronal cells and its promoter is modulated by the POU4 transcription factors. *Molecular Vision*, *19*, 1371–1386.

SUPPORTING INFORMATION

Additional supporting information can be found online in the Supporting Information section at the end of this article.

How to cite this article: Birch, S., & Plachetzki, D. (2023). Multisensory integration by polymodal sensory neurons dictates larval settlement in a brainless cnidarian larva. *Molecular Ecology*, *32*, 3892–3907. https://doi.org/10.1111/mec.16968